

Accurate specimen digitization through glass achieved and validated using 3D surface scanning

Valentin Fischer, Nicolas Vaczi, Rebecca F. Bennion, Romain Cottureau, Jessica Lawrence Wujek, and Jamie A. MacLaren

ABSTRACT

Three-dimensional digitization and morphometric analyses of specimens have become a crucial source of data for natural sciences. However, the quest for thorough sampling has been impaired by exhibition practices of locking specimens behind glass. In this contribution, we tested how well structured white-light scanning and phone-powered photogrammetry (helped with parallel lasers) capture the morphology of a variety of fossil specimens behind modern (i.e., flat) and old (i.e., undulating) glass. Postprocessing of scans was often longer, essentially to remove duplicated surfaces. Nevertheless, we were able to generate precise and accurate meshes through modern glass (validated by scanning objects without the glass): 91–100% of comparable points deviated < 1 mm from the reference model and 89–99% deviated < 0.5 mm. Older glass multiplies the deviations, especially for large, three dimensional specimens. However, these models still have 75 to 94 % of their points deviating less than 0.5 mm from the reference model, which thus remains manageable. We also conducted a linear morphometric analysis on a diagenetically flattened ichthyosaurian and a high-density geometric morphometric analysis of an hippuritid bivalve. The differences in surface digitization techniques (e.g., laser VS structured white-light scanning) and the human error in landmark placement generate more deviation than the presence or absence of glass. We conclude that, with the right scanning methods, specimens can be confidently digitized through glass and incorporated into morphometric (or other digital modelling) analyses.

Valentin Fischer. Evolution & Diversity Dynamics Lab, Université de Liège, 4000 Liège, Belgium (corresponding author). v.fischer@uliege.be

Nicolas Vaczi. Evolution & Diversity Dynamics Lab, Université de Liège, 4000 Liège, Belgium and Département Sciences et Technologies, Haute Ecole en Hainaut, 7000 Mons, Belgium.
nicolasvaczi@gmail.com

Rebecca F. Bennion. Evolution & Diversity Dynamics Lab, Université de Liège, 4000 Liège, Belgium and

Final citation: Fischer, Valentin, Vaczi, Nicolas, Bennion, Rebecca F., Cottureau, Romain, Wujek, Jessica Lawrence, and MacLaren, Jamie A. 2024. Accurate specimen digitization through glass achieved and validated using 3D surface scanning. *Palaeontologia Electronica*, 27(2):a44.

<https://doi.org/10.26879/1375>

palaeo-electronica.org/content/2024/5265-digitisation-through-glass

Copyright: August 2024 Palaeontological Association.

This is an open access article distributed under the terms of the Creative Commons Attribution License, which permits unrestricted use, distribution, and reproduction in any medium, provided the original author and source are credited.

creativecommons.org/licenses/by/4.0

Palaeobiosphere Evolution, Royal Belgian Institute of Natural Sciences, Brussels, Belgium.

rbennionpalaeo@gmail.com

Romain Cottereau. Evolution & Diversity Dynamics Lab, Université de Liège, 4000 Liège, Belgium.

romain.cottereau@uliege.be

Jessica Lawrence Wujek. Physical Sciences Department, Howard Community College, 10901 Little

Patuxent Parkway, Columbia, Maryland, USA. jdlawren@gmail.com

Jamie A. MacLaren. Evolution & Diversity Dynamics Lab, Université de Liège, 4000 Liège, Belgium and

Functional Morphology Lab, Department of Biology, Universiteit Antwerpen, Antwerpen 2610, Belgium.

jamie.maclaren@uantwerpen.be

Keywords: Digitization; 3D; conservation; geometric morphometrics; Ichthyosauria

Submission: 9 February 2024. Acceptance: 24 July 2024.

INTRODUCTION

Specimen digitization technologies such as computed tomography (CT) scanning, photogrammetry, and surface scanning have revolutionised palaeontology (Cunningham et al., 2014). These advances have provided a wealth of accurate three-dimensional (3D) models of ancient phenotypes, enabling unique collections to be digitised for posterity (e.g., Adams et al., 2015; Karim et al., 2016; Davies et al., 2017; Kouraiss et al., 2019; Hedrick et al., 2020) and also facilitating broad scale phenotypic analyses, notably via morphometrics (e.g., Bjarnason and Benson, 2020; Goswami et al., 2022) and biomechanics (e.g., Lautenschlager et al., 2018). However, this quest for digitization can often be impaired by historical specimen exhibition strategies. For example, in the nineteenth century it was popular to mount large blocks containing specimens in wooden boxes, often covered with a glass front. A famous (yet digitizable) example of this style of specimen display is the Marine Reptile Gallery at the Natural History Museum in London, which features over a hundred marine reptiles mounted in glass cases on the walls. Many of these specimens are holotypes and neotypes of ichthyosaurians and plesiosaurians; unfortunately, the glass fronts to the exhibits often renders these vitally important specimens inaccessible for research (Zverkov and Jacobs, 2021). More generally, glass mounts are a ubiquitous feature in many museums worldwide, and many external researchers have already experienced difficulties in having these glass protections removed for research. This severely limits the sampling efforts for studies that require linear measurements and three-dimensional shape, not to mention notable financial drawbacks for researchers travelling long distances and being unable to fully access specimens on arrival.

Finding a way to accurately digitize and scale these specimens would alleviate some of the issues related to (semi-)permanent specimen display. Despite photogrammetry being capable of digitizing images through glass, the method encounters difficulties due to reflections on shiny glass surfaces requiring polarizing filters (Mallison and Wings, 2014), or the lack of ideal lighting conditions (Falkingham, 2012). Here, we test how structured white-light scanning and cameraphone-based photogrammetry accurately captures the morphology of (palaeo)zoological specimens through glass. We test the influence of modern (i.e., flat) and old (i.e., undulating) glass by (i) comparing the deviation of similar points with a reference mesh on a wide range of specimens, from diagenetically flattened ('2.5D') Palaeozoic echinoids to an extant ibex skull (full 3D), and by (ii) applying and comparing linear and high-density geometric morphometric methods on two case studies (an Early Jurassic ichthyosaurian and a Cretaceous rudist, respectively). Moreover, we showcase a device we designed for projecting a laser scale onto specimens through glass, allowing accurate scaling of pictures and 3D meshes obtained through photogrammetry. This quantification of error from different 3D surface digitization methods goes hand-in-hand with a call for transparency in reporting protocols, errors, and inaccuracies, as well as establishing consistent good practice in specimen digitization (Davies et al., 2017; Díez Díaz et al., 2021).

MATERIALS AND METHODS

Sampling, Photographing, and Scanning

We sampled a series of 11 extinct and extant metazoan specimens spanning a broad range of colours, geometries, and diagenetic alterations

(Table 1) from the fossil collections of the Université de Liège (Belgium, institutional abbreviation ULgPA). Each of these specimens was scanned with a structured white-light scanner with a broad field of view (Artec Eva, precision ≈ 0.5 mm) and with a more precise scanner, to allow comparisons between digitization method in addition to the presence of glass (either a structured white-light scanner with a narrow field of view [Artec Spider, precision ≈ 0.2 mm] or a laser scanner [Creaform Handyscan 300, precision = 0.2 mm]). All specimens were then scanned through two types of glass (a recent, flat glass and an older, undulating (blowglass-like) glass) using the white-light scanners (Figure 1). Specimens were placed approximately 150 mm from the glass and both kinds of glass have the same thickness, about 0.5 mm. Two specimens (a hyena skull ULgPA1806 and a juvenile ichthyosaurian ULgPA13413) were scanned through thicker, horizontal showcase glass; this replicated another kind of museum setup. Each structured light scan was processed using the automated parameters in Artec Studio v17, with the following procedure: cleaning, alignment, global registration, merging, meshing, mesh simplification. Holes in the mesh surface were automatically closed if < 5 mm and left open otherwise. Laser scans were processed with Creaform VxElements

v11 (aligning, merging, meshing). Holes in the mesh surface were automatically closed if small and left open otherwise. Errors and difficulties in digitization are discussed (Figure 2, see below).

Photogrammetric models were generated for two specimens (a rudist bivalve ULgPA3727 and a juvenile ichthyosaurian preserved on a slab. ULgPA13413). We took ~ 35 pictures around the rudist specimen, and ~ 50 for the ichthyosaurian, in each setting (air/reference + modern glass + old glass for the rudist, and air/reference + horizontal glass for the ichthyosaurian). Images were taken with a 12 MP camera mounted within an iPhone 11 pro. By current standards this has a fairly low resolution and would directly affect the quality of the models produced. However, our goal here is to test the effect of using affordable methods available to any researcher worldwide as well as compare these results to those obtained using professional-grade scanners. Pictures were imported in Reality Capture v1.2 (RC © Epic Games Slovakia), and surface meshes were created using the standard, automated procedure without control points or ground controls (Import Inputs > Align Images > Calculate Model [Normal quality] > Texturise > Colourize [Normal quality]). We then manually removed triangles created in poorly visible areas, so that only reliable surfaces were compared to

TABLE 1. Specimen sampling, with basic information on size, colour, and shape.

Taxon	Specimen	Size	Colour	Flattened?	Scanner used
<i>Crocota crocuta spelaea</i> (Mammalia)	ULgPA1806, cranium	262 mm	Light brown	No	Artec Eva
<i>Hippurites radiosus</i> (Hippuritida)	ULgPA3727, complete shells	158 mm	Beige	No	Artec Eva, Artec Spider
<i>Ursus spelaeus</i> (Mammalia)	ULgPA12766, femur	486 mm	Brown	No	Artec Eva
<i>Ichthyosaurus</i> sp. (Reptilia)	ULgPA13413, complete skeleton	1044 mm	Dark grey	Yes	Artec Eva, Creaform Handyscan
<i>Pleurosaurus thiollieri</i> (Reptilia)	ULgPA25056, cast of complete skeleton	808 mm	Brown	Yes	Artec Eva
<i>Proterocidaris</i> sp. (Echinoidea)	ULgPA35400, complete test	196 mm	Black	Yes	Artec Eva
<i>Lovenechinus</i> sp. (Echinoidea)	ULgPA35401, complete test	174 mm	Black	Moderately	Artec Eva, Creaform Handyscan
<i>Siphonophyllia cylindrica</i> (Rugosa)	ULgPA20230303-4, complete skeleton	136 mm	Light brown	No	Artec Eva
<i>Caninophyllum patulum</i> (Rugosa)	ULgPA20230303-5, complete skeleton	112 mm	Light brown	Mostly no	Artec Eva
<i>Capra hircus</i> (Mammalia)	ULgPA20230320-1, cranium	393 mm	Light beige	No	Artec Eva

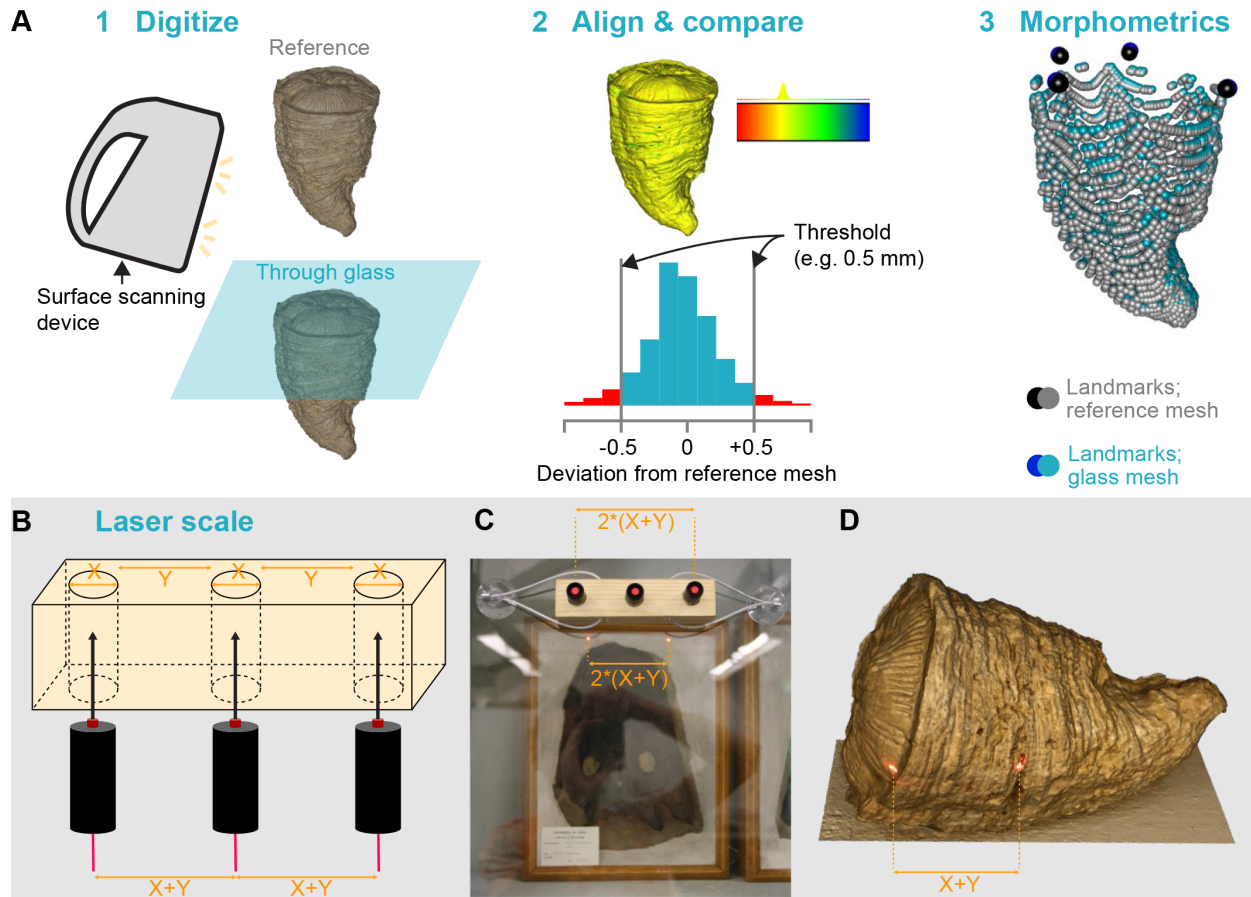


FIGURE 1. Protocols employed in this paper. (A) protocol for assessing the performance of surface scanning through glass. (B) schematics of the laser scaling device we describe in this paper. (C) photograph of the laser scaling device in action. (D) photogrammetric model of an hippuritid bivalve showing the laser dots clearly visible on the model texture.

one another to assess mesh deviations. Scanning and photogrammetry were performed in the exact same location with constant lighting conditions (overcast conditions with neon lighting from above).

Laser Scaling Device

Scaling specimens is a cornerstone of photogrammetry and is strongly compromised when specimens are locked behind glass. We solved this by creating ‘Scale3000’, a device projecting parallel lasers onto the specimen, perpendicular to the glass, with the beams separated by a known distance (Figure 1B). Because the beam is set perpendicular to the glass, we estimate that the deviation of the beam is negligible. We confirm this by analysing centroid size differences in 3D geometric morphometrics (see below). This device is a modification from what has been used in ecological studies aiming to estimate the size of animals in

the wild (Bergeron, 2007; Rothman et al., 2008; Rohner et al., 2011); the main advantage of our method is that it does not require the researcher to know the lens focal length nor the distance from the object being studied. Further technical details on Scale3000 will be published online after publication of the paper.

Analyses of Mesh Deviations

The resultant models were aligned in Artec Studio v17 (although alignment can also be done in a freeware of choice, such as MeshLab or CloudCompare) and were reexported as .stl files. These meshes were imported in pairs (for example reference mesh + modern glass mesh) in the open source software CloudCompare v2.13.alpha (<http://www.cloudcompare.org>) (Figures 1, 3, 4). Meshes were then finely registered, allowing optimal overlap and alignment (root mean square difference set at the default value of 10^{-5}). We then computed the

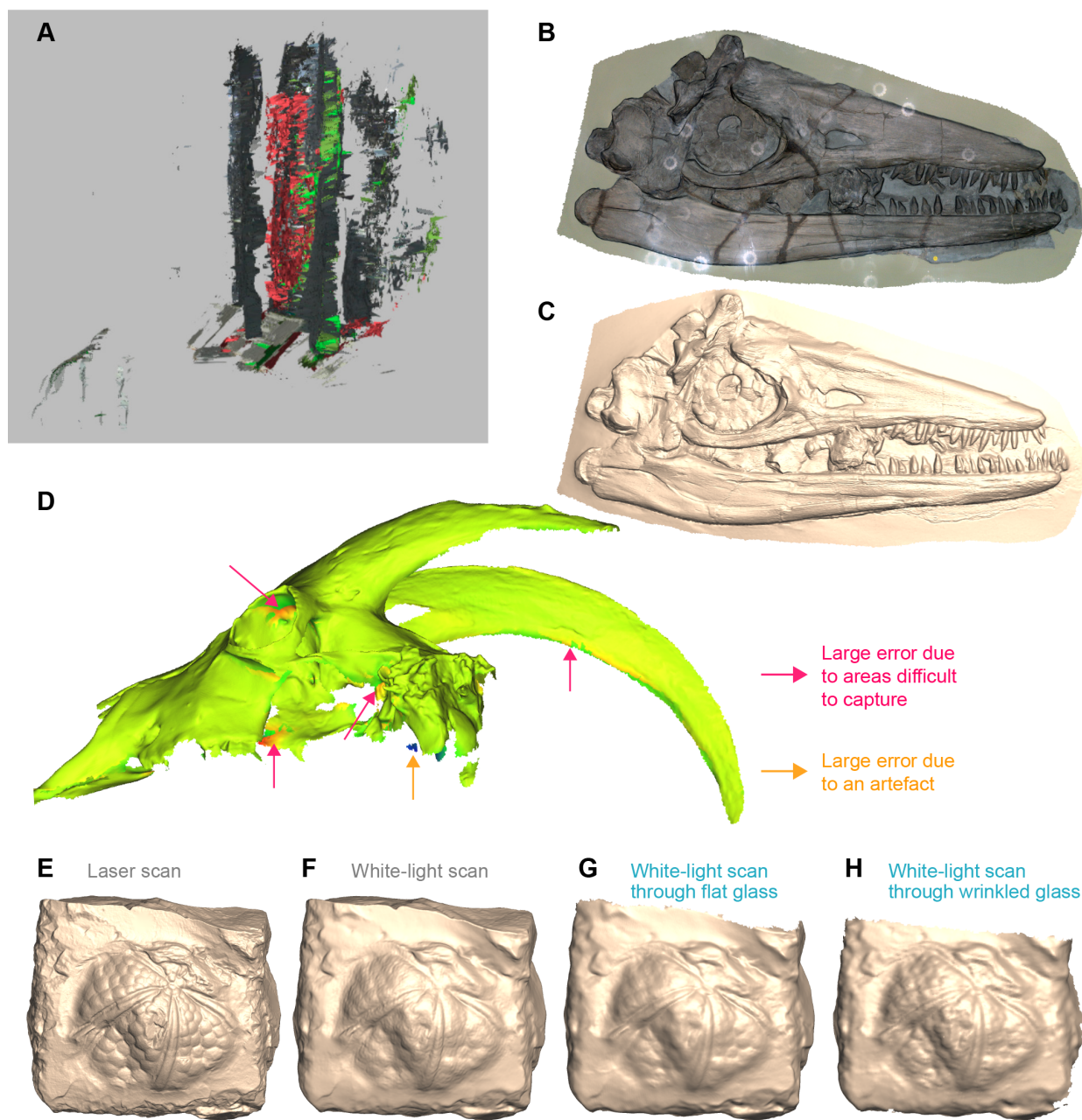


FIGURE 2. Difficulties and issues in data acquisition. (A) multiple surfaces created by reflections on the glass; these are frequent when using scanners requiring a close distance from the specimen, such as the Artec Spider. (B) light rings polluting the texture of the final model of NHMUK R1157, holotype of *Temnodontosaurus eurycephalus*. The 3D mesh (C) appears detailed, nonetheless. (D) 3D mesh of the extant goat ULgPA20230320-1, showing important errors in the orbit, palate, and basicranium. (E–H) 3D meshes of *Lovenechinus* sp. (ULgPA35401) produced using laser scanning with Creaform Handyscan 300 (E), white-light scanning with Artec Eva (F), white-light scanning with Artec Eva through flat glass (G), white-light scanning with Artec Eva through old glass (H), showing progressively fewer details of minute anatomical structures.

cloud/mesh (C2M) distance, using the default parameters (signed distances, multi-threaded), and exported the histogram data of the signed distances for processing and visualisation in R v.4.2.1 (Table 2).

Morphometrics

Deviation from a reference model offers a good estimation of the effect of digitization technique or settings on 3D model accuracy. However,

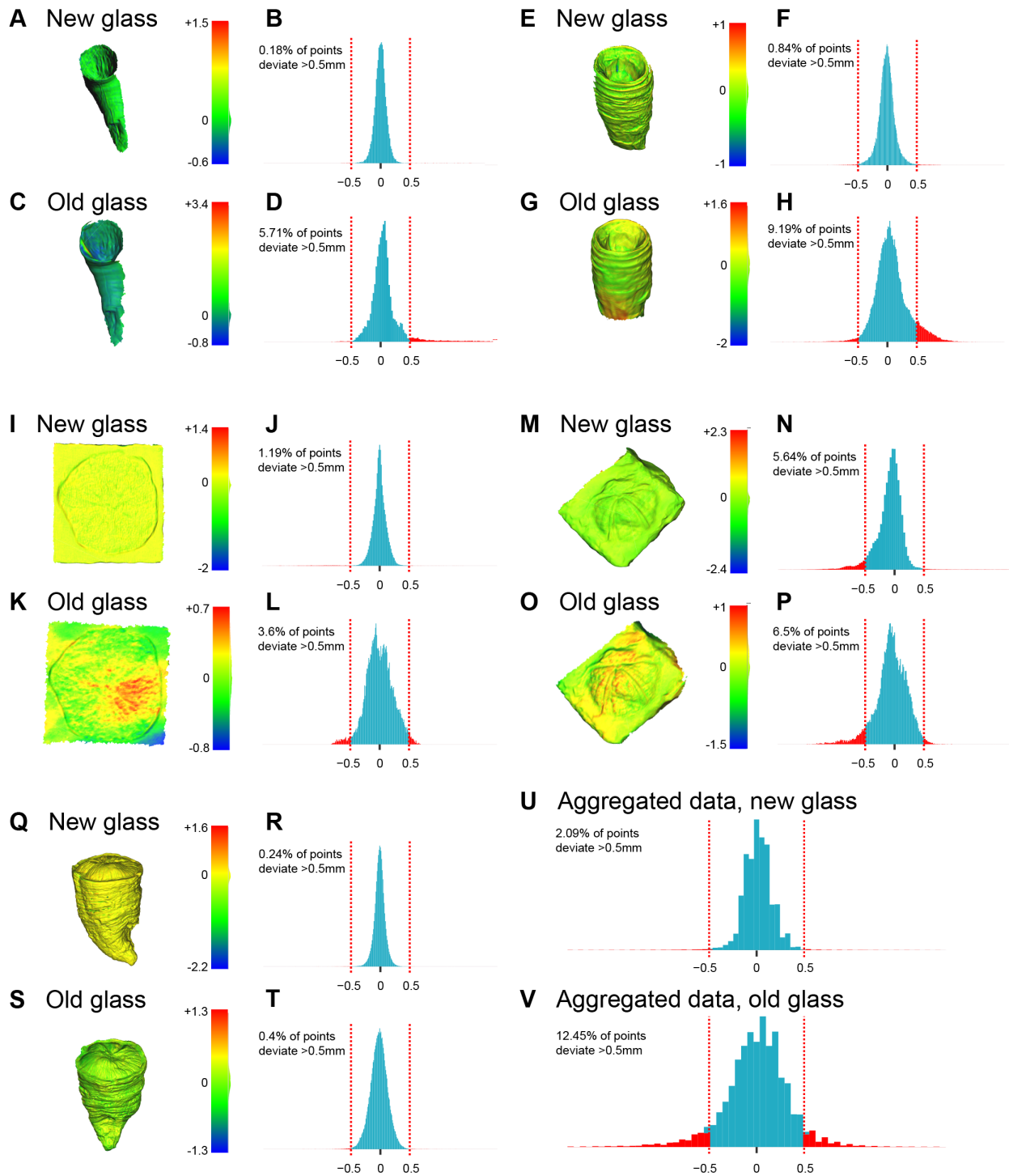


FIGURE 3. Mesh deviations from reference (laser scanned without glass), invertebrate fossils. (A–D) *Caninophyllum patulum* (ULgPA20230303-5); mapping of deviations (A, C) and associated histograms (B, D). (E–H) *Siphonophyllia cylindrica* (ULgPA20230303-4); mapping of deviations (E, G) and associated histograms (F, H). (I–L) *Proterocidaris* sp. (ULgPA35400); mapping of deviations (I, K) and associated histograms (J, L). (M–P) *Lovenechinus* sp. (ULgPA35401); mapping of deviations (M, O) and associated histograms (N, P). (Q–T) *Hippurites radiosus* (ULgPA3727); mapping of deviations (Q, S) and associated histograms (R, T). (U, V) aggregated data (invertebrates and vertebrates) for new (Q) and old (V) glass.

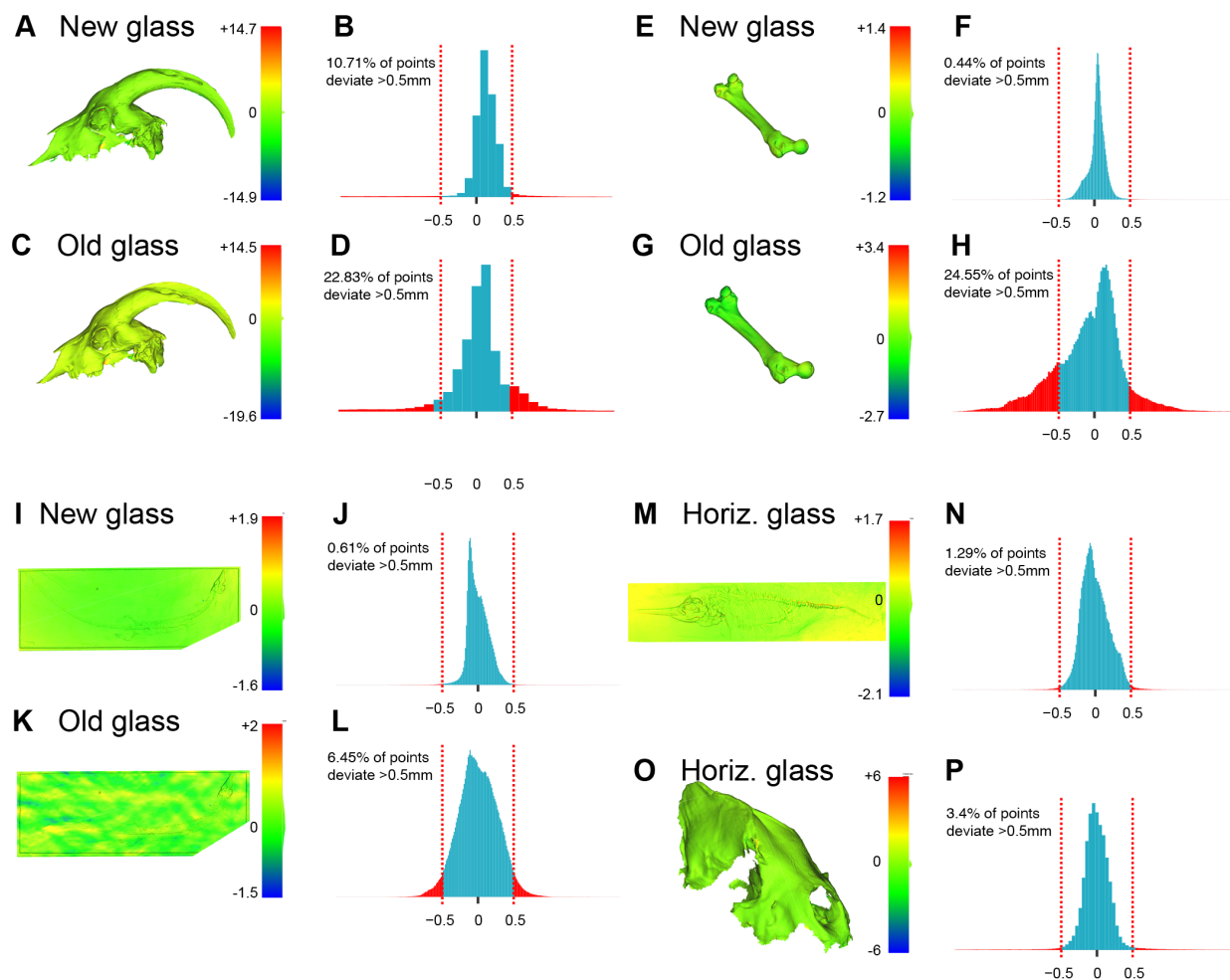


FIGURE 4. Mesh deviations from reference (laser scanned without glass), vertebrate fossils. (A–D) skull of *Capra hircus* (ULgPA20230320-1); mapping of deviations (A, C) and associated histograms (B, D). (E–H) femur of *Ursus spelaeus* (ULgPA12766); mapping of deviations (E, G) and associated histograms (F, H). (I–L) cast of *Pleurosaurus thiollieri* (ULgPA25056); mapping of deviations (I, K) and associated histograms (J, L). (M–N) *Ichthyosaurus* sp. (ULgPA13413); mapping of deviations (M) and associated histogram (N). (O–P) skull of *Crocota crocota spelaea* (ULgPA1806); mapping of deviations (O) and associated histogram (P). Abbreviation: horiz, horizontal.

it is also important to understand the effect that scanning through glass might have on morphometric measurements. Indeed, many morphometric studies employ Z-transformed ratios or two/three-dimensional XY(Z) coordinates as measures of shape or form, which will then be subjected to a Procrustes superimposition, reducing the need to have highly accurate estimates of absolute size. It is thus valuable to understand the effect of digitizing through glass in these ‘real-life’/applied scenarios such as linear and geometric morphometric studies.

To examine the effect on linear morphometrics and functional ratios, we recorded linear measurements on the skull and teeth of the ichthyosaurian ULgPA13413 (*Ichthyosaurus* sp.) on meshes

obtained via: Artec Eva, Artec Eva through horizontal glass, Handyscan300 (laser scanner, 0.2 mm precision), and photogrammetry. Measurements taken followed the method of Bennion et al. (2022) (see Tables 3,4, Figure 5). We compared the deviations introduced by scanning method (laser VS white-light- against those induced by the presence of glass (white-light VS white-light behind glass) using a Wilcoxon two-sample test. A single operator (VF) did all the measurements to avoid the interoperator bias.

To assess the effect on geometric morphometric data acquisition, we applied a semi-automated high-density surface landmarking protocol (after Fischer et al., 2022) on the external surface of the right valve of the rudist ULgPA3727 (*Hippur-*

TABLE 2. Effect of glass (new and old) in deviating points compared to the reference mesh. All specimens compared here have been scanned with an Artec Eva.

	New glass, points with < 0.5 mm deviation (%)	New glass, points with < 1 mm deviation (%)	Old glass, points with < 0.5 mm deviation (%)	Old glass, points with < 1 mm deviation (%)
ULgPA12766 <i>Ursus spelaeus</i> femur	99.56	99.97	75.45	94.69
ULgPA13413 <i>Ichthyosaurus</i> sp.	98.71	99.95	NA	NA
ULgPA1806 <i>Crocota crocuta spelaea</i> skull	96.6	98.32	NA	NA
ULgPA20230303-4 <i>Siphonophyllia cylindrica</i>	99.16	100	90.81	99.52
ULgPA20230303-5 <i>Caninophyllum patulum</i>	99.82	99.95	94.29	97.45
ULgPA20230320-1 <i>Capra hircus</i> skull	89.29	91.74	77.17	88.38
ULgPA25056 <i>Pleurosauros thiollieri</i> (cast)	99.39	99.92	93.55	99.91
ULgPA35400 <i>Proterocidaris</i> sp.	98.81	99.53	96.4	100
ULgPA35401 <i>Lovenechinus</i> sp.	94.36	98.88	93.5	99.4
ULgPA3727 <i>Hippurites radiosus</i>	99.76	99.96	99.6	99.98
MIN	89.29	91.74	75.45	88.38
MAX	99.82	100	99.6	100

TABLE 3. Raw measurements taken on each mesh generated from specimen ULgPA13413. Laser scans were used as a control and were performed with no glass between scanner and object.

Mesh	Mandible length	Skull length	Snout length	Snout depth	Orbit length	Articular to coronoid	Articular to retroarticular	Crown diameter	Crown height
Laser	264.304	257.67	159.27	6.77	48.08	18.48	12.46	4.51	2.53
Eva	266.8	262.1	164.87	5.52	47.75	20.38	15.82	4.64	2.99
Glass horizontal	265.83	261.86	162.9	7.05	46.04	20.05	15.01	4.26	3.5

TABLE 4. Morphological ratios computed on the raw data (Table 3) for each mesh generated from specimen ULgPA13413.

Mesh	Tooth shape	Absolute crown size	Relative orbit size	Relative snout length	Relative snout depth	Anterior mechanica advantage	Opening mechanical advantage
Laser	0.56097561	2.53	0.186595257	0.618116195	0.042506436	0.069919487	0.047142684
Eva	0.644396552	2.99	0.182182373	0.62903472	0.033480924	0.076386807	0.059295352
Glass horizontal	0.821596244	3.5	0.17581914	0.622088139	0.043278085	0.075424143	0.056464658

ites radiosus). The sequence of fixed landmarks is as follows (Figure 5): 1, extremity of the attached valve; 2, commissure (valve junction), deepest longitudinal groove on the posterior surface; 3, commissure, anteroventral extremity of a trapezoidal

boss on the anterior surface; 4, commissure, small, damaged arch on the dorsal surface; 5: commissure, small groove on the ventral surface. This landmarking scheme was applied to meshes obtained via: Artec Eva, Artec Spider, Artec Spider

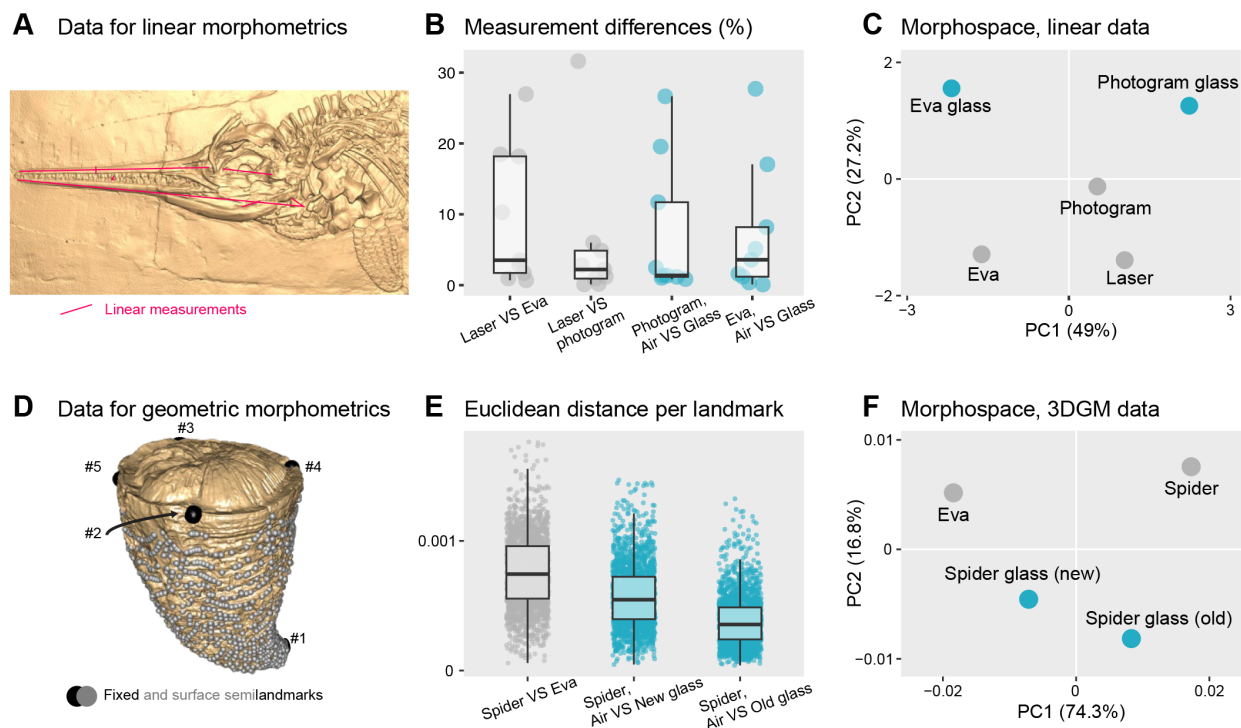


FIGURE 5. Case studies of morphometric analyses (A–C linear morphometrics; D–F high-density 3D geometric morphometrics). (A) 3D mesh of *Ichthyosaurus* sp. (ULgPA13413) produced by laser scanning showing the traits (linear measurements) we took. (B) relative differences in measurement lengths for each trait, comparing methods (grey) and the presence of glass (blue). (C) morphospace resulting from Principal Component Analysis of the z-transformed trait data. (D) 3D mesh of *Hippurites radiosus* (ULgPA3727) produced by white-light scanning, with fixed (black) and automatically placed surface semi-landmarks (grey) superimposed. (E) euclidean distance per landmark, comparing methods (grey) and the presence of new and old glass (blue). (F) morphospace resulting from Principal Component Analysis of the Procrustes coordinates.

through modern glass, and Artec Spider through old glass, with fixed landmarks placed using StratoVan Checkpoint v.20.10.13.0859. These landmarks were exported as .pts files and imported into R for semi-automated surface semi-landmark placement; 2000 surface semi-landmarks were used with a dome-shaped atlas mesh (see the protocol in Fischer et al. (2022)). These fixed and surface semi-landmarks were submitted to a Generalised Procrustes Superimposition and visualised via a principal component analysis.

Data Availability

We place all our data and scripts in the Institutional repository of the Université de Liège (orbi.uliege.be). This includes: (i) the 3D template and landmarks for high-density 3D landmarking; (ii) a dataset of linear measurements on a specimen of *Ichthyosaurus*; (iii) the R script to generate histograms from CloudCompare data; (iv) the R script for running high-density 3D geometric morphometrics; (v) all 3D models. Supporting data for this

paper are available for download as Supplementary Data at <https://palaeo-electronica.org/content/2024/5265-digitisation-through-glass>.

RESULTS

Digitization Process

Capturing surface data through glass can be challenging. It was often impossible to obtain quality data with the more precise scanner (Artec Spider; Figure 2). There are two reasons for this: (i) it requires a close distance to the object and the ≈ 150 mm distance between the object and the glass made it impractical to use, and (ii) it was often interpreting glass reflections as relevant shapes, creating parallel and often imbricated surfaces that are difficult to clean up. In the worst cases, this produced partially distorted copies of the target surface, overlapping the genuine data (Figure 2), and thus required painstaking cleaning. This was rare with the structured white-light scanner with a larger field of view, which requires a lon-

ger distance from the object (Artec Eva), and therefore most results focus on the meshes obtained by this scanner. Another minor issue observed was that when scanning perpendicular to the glass, flashes sometimes appeared on the texture of the models (Figure 2). While this reduced the amount of detail which could be extracted from the texture, such as minute bone sutures, the effect did not appear to influence the quality of the mesh (Figure 2), only the colouration of the resultant surface.

Additionally, an effect of scanning method distinct from the XYZ placement of landmark points was the precision of the model; precision describes the ability for the digitization method to capture minute details of the object in the resultant digital version. We found that scanning through glass, especially undulating glass, generated less precise models (Figure 2), where the boundaries between anatomical elements became less perceptible. However, the effect of glass was less marked than differences generated by different scanning technologies (Figure 2) (see also Díez Díaz et al., 2021).

Mesh Deviations

The presence of modern, flat glass between subject and scanner/camera resulted in accurate meshes, where a high percentage (89.3–99.8%) of the points deviated from the reference model by less than 0.5 mm (Figures 3, 4; Table 2); 0.5 mm was the limit of detection of the scanner we used for most of these analyses (Artec Eva; Table 1). If a threshold of 1 mm is selected instead, this proportion of accurate meshes digitised behind modern glass increased to 91.7–100% (Figures 3, 4; Table 2). When considering different object shapes, the worst results by far were those obtained from the extant goat skull, which is a fully 3D object (*Capra hircus*; ULgPA20230320-1). Problematic points were not distributed randomly but were found in areas that were difficult to reach without a marked angle (e.g., the inside surface of the orbit, the palate, the ventrolateral surface of the basicranium; Figure 2). Scanning with a strong angle increased reflections, and this reduced the data gathered in these areas, producing less accurate surfaces. Our aggregated results, taking all the points measured, recover a mean of 2% points deviating for more than 0.5 mm (Figure 3).

The effect of older, undulating, blown glass were more difficult to predict. Generally, this kind of glass multiplied the deviations; the percentage of points deviating more than the thresholds was sim-

ilar, often multiplied by a factor of 1.5–3, but sometimes much higher (up to 177 times higher; Table 2). Two specimens skewed this high proportion of inaccurate points when scanned through undulating glass (instead of flat glass): the cave bear femur (*Ursus spelaeus*; ULgPA12766) and the extant goat skull (*Capra hircus*; ULgPA20230320-1). The femur was a long object (493 mm long) and was purposefully placed obliquely with respect to the glass to mimic possible arrangement in museums. As a result, some parts of the specimen were closer and easier to capture by circling in front of the specimen, while the range of angles we could use to scan the most remote parts were smaller, resulting in less accurate data. Still, while 24.75% (100–75.25%) of points deviated by more than 0.5 mm compared to the reference mesh, this metric of inaccuracy dropped to 3.31% when a threshold of 1 mm was selected instead (Table 2). Aggregated data found 12.45% of the points deviated by more than 0.5 mm (Figure 3).

Morphometrics

The biggest challenge faced was the accurate placement of points for linear measurements or fixed-point landmarks. This was due to the fact that some digitization methods (white-light vs. laser scanning) and older glass reduced the precision of the model (Figure 2), making it more difficult to pinpoint small anatomical structures with precision. As a result, greater human error was induced in measurements and landmark placement, with this error being linked to the scanning technique used. We provide the raw measurements and the linear morphometric ratios obtained from multiple meshes generated on the ichthyosaurian specimen in Tables 3 and 4, respectively. The average deviation of the ratios is roughly $\leq 5\%$ for both the laser vs. white-light comparison and the air vs. (horizontal) glass comparison (Figure 5; Table 4). A Wilcoxon two-sample test did not regard either of these sets of deviations as significantly distinct from one another (p -value = 0.6048). Nevertheless, a couple of ratios deviated more notably ($>15\%$); this appeared to be the case more frequently for comparisons between scanning methods rather than for comparisons between the presence or absence of glass (Figure 5). The morphospace resulting from a Principal Component Analysis of these linear ratios also recovers a stronger influence of the scanning methods (oriented along the first axis, which accounted for 48.95% of the total variance), whereas the presence of glass was essentially represented along

the second axis (accounting for 27.2% of the total variance).

The picture was similar for high-density three-dimensional morphometrics. The Euclidean distance per fixed and surface semi-landmarks was larger in between scanning techniques (laser vs. white-light) than for the presence of glass (Figure 5). Our two-sample Wilcoxon test recovered the methods (laser vs. the two white-light populations combined) and the type of glass (white-light new glass vs. white-light old glass) as significantly distinct (p -value < 0.001 in both cases). Perhaps counterintuitively, the distance in landmark placements between the reference mesh and the mesh generated through glass appeared slightly smaller through old glass compared to new glass (Figure 5), possibly indicating a stronger influence of human error than mesh shape differences. In any case, these differences were very small; the maximal difference in centroid size was 0.64%, also possibly reflecting human error in the placement of fixed landmarks. The resulting morphospace was similar to the one generated for our linear morphometric case study, in the sense that the scanning methods (white-light with Artec Eva vs. white-light with Artec Spider) form the extremes of the first axis of the Principal Coordinate Analysis (accounting for 74.3% of the total variance) and the presence of glass structures the second axis (accounting for 16.8% of the total variance) (Figure 5).

DISCUSSION AND CONCLUSIONS

Can We Efficiently Digitize an Object Through Glass?

Our assessment of the capabilities of structured white-light surface scanning and photogrammetry through glass is reassuring: the presence of flat glass is not distorting specimens and accurate models can be generated with minor deviations from the original specimen. Older 'blown' glass, with its undulating surface, creates more deviations, which are sometimes manageable, sometimes above the precision threshold we used in some of our previous studies (i.e., scans with precisions of 0.2–0.6 mm) (e.g., MacLaren et al., 2022; Fischer et al., 2022). Our results nevertheless suggest that the scanning method (see also Díez Díaz et al., 2021) and the human error in landmark/anatomical point placement are bigger factors in driving morphometric differences than the presence of glass (see also Von Cramon-Taubadel et al., 2007; Shearer et al., 2017). Accordingly, we provide a

decision tree to help anyone requiring a 3D model of (palaeo)biological specimens to assess whether a scan through glass is sensible and usable in quantitative studies (Figure 6). The key things to check and to plan are:

1. Check glass reflections at a $\approx 30^\circ$ angle and estimate specimen distance from the glass.
2. Does your study require a precision < 1 mm, < 0.5 mm ?
3. Are key areas for your study well exposed and thus scannable at multiple angles?
4. Does your study require a full, detailed texture to place landmarks/measure traits?

The cost of handheld scanners, in addition to the cost of their associated software packages and computers with the required capabilities, is restrictive. Photogrammetry offers a cheaper alternative, using open source software which can be run on increasingly lower-cost devices (e.g., Falkingham, 2012). Furthermore, this technique of creating surface 3D models has already been shown to be especially useful for museum gallery specimens with access difficulties other than glass (e.g., large

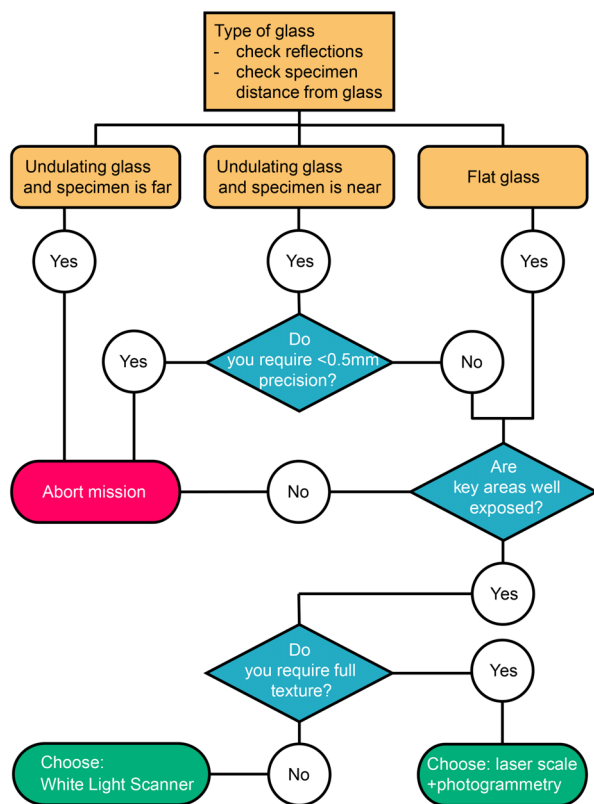


FIGURE 6. Decision tree to assess the usefulness and select the 3D digitization method when specimens are behind glass.

mounted skeletons) (Fau et al., 2016). The laser-scale device outlined in this study adds to the potential uses of photogrammetry in museum settings as it provides an affordable solution to researchers who require 3D model data or measurements from behind glass.

The Importance of Physical Access to Specimens

As outlined in our workflow above, 3D scanning is not always an appropriate method for obtaining data from specimens behind glass. This can particularly be the case where specimens are preserved in three dimensions with areas invisible or poorly visible by the scanning device or with areas that are obscured by the wooden edges of the display case. Our results found that areas of the specimen which require strong angles (with respect to the orthogonal of the glass plane) to scan were more susceptible to errors. In these situations, it is preferable for the specimen to be removed for scanning.

Despite the ongoing revolution of 3D morphology studies, surface digitizing will always create an imperfect and partial model of the original specimen. Surface digitizing does not usually capture the entirety of the specimen and usually leave gaps, most notably when attempted through glass. Physical access to specimens is mandatory as many types of analysis rely on data not capturable by surface digitizing. These notably include taxonomy, comparative anatomy, phylogenetic analyses (always requiring detailed interpretation of minute bony sutures and structures), detection of patholo-

gies, and feeding ecology, which relies on minute structure and wear patterns on tooth crown enamel (e.g., Massare, 1987; Schubert and Ungar, 2005; Bennion et al., 2023). Some other lines of research require samples which can only be gathered physically from the specimen, such as moulds for tooth microwear analysis (e.g., Purnell et al., 2017; Bestwick et al., 2020) and bone histology and microanatomy (e.g., Houssaye, 2013). Finally, physical access is also crucial to assess the authenticity of specimens; it is well known that many historical specimens (with a single accession number) have been artificially enhanced, sometimes even creating chimera (McGowan, 1990; Massare and Lomax, 2016; Rossi et al., 2024). Therefore, it is vital that the protocol outlined and tested in this study is not used by institutions to restrict physical access to specimens by external individuals. Rather, it offers options to museums and researchers faced with logistical difficulties.

ACKNOWLEDGEMENTS

We thank S. Chapman, Z. Hughes, and R. Hansen (NHMUK) for facilitating RFB and JLW's visits. We also thank A. Caps for his help with scanning ULiege's fossil collections. Finally, we thank editor Lucia Smidova, Dr. Verónica Díez-Díaz, and one anonymous reviewer for helping us shape the paper with thoughtful comments and suggestions. RFB was funded by F.R.S.-FNRS FRIA PhD Fellowship (grant number FC 23645) and JAM and VF by F.R.S.-FNRS Project SEASCAPE when this research was conducted.

REFERENCES

- Adams, J.W., Olah, A., McCurry, M.R., and Potze, S. 2015. Surface Model and Tomographic Archive of Fossil Primate and Other Mammal Holotype and Paratype Specimens of the Ditsong National Museum of Natural History, Pretoria, South Africa. PLOS ONE 10:e0139800. Public Library of Science. <https://doi.org/10.1371/journal.pone.0139800>
- Bennion, R.F., MacLaren, J.A., Coombs, E.J., Marx, F.G., Lambert, O., and Fischer, V. 2022. Convergence and constraint in the cranial evolution of mosasaurid reptiles and early cetaceans. *Paleobiology*, 1–17. <https://doi.org/10.1017/pab.2022.27>
- Bennion, R.F., Maxwell, E.E., Lambert, O., and Fischer, V. 2023. Craniodental ecomorphology of the large Jurassic ichthyosaurian *Temnodontosaurus*. *Journal of Anatomy*, joa.13939. <https://doi.org/10.1111/joa.13939>
- Bergeron, P. 2007. Parallel Lasers for Remote Measurements of Morphological Traits. *The Journal of Wildlife Management*, 71:289–292. <https://doi.org/10.2193/2006-290>

- Bestwick, J., Unwin, D.M., Butler, R.J. and Purnell, M.A. 2020. Dietary diversity and evolution of the earliest flying vertebrates revealed by dental microwear texture analysis. *Nature Communications*, 11:1–9. Springer US.
<https://doi.org/10.1038/s41467-020-19022-2>
- Bjarnason, A. and Benson, R. 2020. A 3D geometric morphometric dataset quantifying skeletal variation in birds. *M3 Journal* 7:1–10.
<https://doi.org/10.18563/journal.m3.125>
- Cunningham, J.A., Rahman, I.A., Lautenschlager, S., Rayfield, E.J. and Donoghue, P.C.J. 2014. A virtual world of paleontology. *Trends in Ecology & Evolution*, 29:347–357.
<https://doi.org/10.1016/j.tree.2014.04.004>
- Davies, T.G., Rahman, I.A., Lautenschlager, S., Cunningham, J.A., Asher, R.J., Barrett, P.M., Bates, K.T., Bengtson, S., Benson, R.B.J., Boyer, D.M., Braga, J., Bright, J.A., Claessens, L.P.A.M., Cox, P.G., Dong, X.P., Evans, A.R., Falkingham, P.L., Friedman, M., Garwood, R.J., Goswami, A., Hutchinson, J.R., Jeffery, N.S., Johanson, Z., Lebrun, R., Martínez-Pérez, C., Marugán-Lobón, J., O'Higgins, P.M., Metscher, B., Orliac, M., Rowe, T.B., Rücklin, M., Sánchez-Villagra, M.R., Shubin, N.H., Smith, S.Y., Starck, J.M., Stringer, C., Summers, A.P., Sutton, M.D., Walsh, S.A., Weisbecker, V., Witmer, L.M., Wroe, S., Yin, Z., Rayfield, E.J., and Donoghue, P.C.J. 2017. Open data and digital morphology. *Proceedings of the Royal Society B: Biological Sciences*, 284.
<https://doi.org/10.1098/rspb.2017.0194>
- Díez Díaz, V., Mallison, H., Asbach, P., Schwarz, D., and Blanco, A. 2021. Comparing surface digitization techniques in palaeontology using visual perceptual metrics and distance computations between 3D meshes. *Palaeontology*, 64:179–202.
<https://doi.org/10.1111/pala.12518>
- Falkingham, P. 2012. Acquisition of high resolution three-dimensional models using free, open-source, photogrammetric software. *Palaeontologia Electronica*, 15:1–15.
<https://doi.org/10.26879/264>
- Fau, M., Cornette, R., and Houssaye, A. 2016. Photogrammetry for 3D digitizing bones of mounted skeletons: Potential and limits. *Comptes Rendus Palevol*, 15:968–977.
<https://doi.org/10.1016/j.crpv.2016.08.003>
- Fischer, V., Bennion, R.F., Foffa, D., MacLaren, J.A., McCurry, M.R., Melstrom, K.M., and Bardet, N. 2022. Ecological signal in the size and shape of marine amniote teeth. *Proceedings of the Royal Society B: Biological Sciences*, 289:20221214.
<https://doi.org/10.1098/rspb.2022.1214>
- Goswami, A., Noirault, E., Coombs, E.J., Clavel, J., Fabre, A.-C., Halliday, T.J.D., Churchill, M., Curtis, A., Watanabe, A., Simmons, N.B., Beatty, B.L., Geisler, J.H., Fox, D.L., and Felice, R.N. 2022. Attenuated evolution of mammals through the Cenozoic. *Science*, 378:377–383.
<https://doi.org/10.1126/science.abm7525>
- Hedrick, B.P., Heberling, J.M., Meineke, E.K., Turner, K.G., Grassa, C.J., Park, D.S., Kennedy, J., Clarke, J.A., Cook, J.A., Blackburn, D.C., Edwards, S.V., and Davis, C.C. 2020. Digitization and the Future of Natural History Collections. *BioScience* 70:243–251.
<https://doi.org/10.1093/biosci/biz163>
- Houssaye, A. 2013. Bone histology of aquatic reptiles: what does it tell us about secondary adaptation to an aquatic life? *Biological Journal of the Linnean Society*, 108:3–21.
<https://doi.org/10.1111/j.1095-8312.2012.02002.x>
- Karim, T., Burkhalter, R., Farrell, Á., Molineux, A., Nelson, G., Utrup, J., and Butts, S. 2016. Digitization workflows for paleontology collections. *Palaeontologia Electronica*, 19.3.4T: 1-14.
<https://doi.org/10.26879/566>
- Kouraiss, K., El Hariri, K., El Albani, A., Azizi, A., Mazurier, A., and Lefebvre, B. 2019. Digitization of Fossils from the Fezouata Biota (Lower Ordovician, Morocco): Evaluating Computed Tomography and Photogrammetry in Collection Enhancement. *Geoheritage*, 11:1889–1901.
<https://doi.org/10.1007/s12371-019-00403-z>
- Lautenschlager, S., Gill, P.G., Luo, Z.-X., Fagan, M.J., and Rayfield, E.J. 2018. The role of miniaturization in the evolution of the mammalian jaw and middle ear. *Nature*, 561:533–537.
<https://doi.org/10.1038/s41586-018-0521-4>

- MacLaren, J.A., Bennion, R.F., Bardet, N., and Fischer, V. 2022. Global ecomorphological restructuring of dominant marine reptiles prior to the K/Pg mass extinction. *Proceedings of Royal Society B*, 289:20220585.
<https://doi.org/rspb.2022.0585>
- Mallison, H. and Wings, O. 2014. Photogrammetry in paleontology – a practical guide. *Journal of Paleontological Techniques*, 12:1–31.
- Massare, J.A. 1987. Tooth morphology and prey preference of Mesozoic marine reptiles. *Journal of Vertebrate Paleontology*, 7:121–137.
- Massare, J.A. and Lomax, D.R. 2016. Composite skeletons of *Ichthyosaurus* in historic collections. *Paludicola* 10:207-240.
- McGowan, C. 1990. Problematic Ichthyosaurs from Southwest England: a question of authenticity. *Journal of Vertebrate Paleontology*, 10:72–79.
- Purnell, M.A., Goodall, R.H., Thomson, S., and Matthews, C.J.D. 2017. Tooth microwear texture in odontocete whales: variation with tooth characteristics and implications for dietary analysis. *Biosurface and Biotribology*, Elsevier Inc.
<https://doi.org/10.1016/j.bsbt.2017.11.004>
- Rohner, C.A., Richardson, A.J., Marshall, A.D., Weeks, S.J., and Pierce, S.J. 2011. How large is the world's largest fish? Measuring whale sharks *Rhincodon typus* with laser photogrammetry. *Journal of Fish Biology*, 78:378–385.
<https://doi.org/10.1111/j.1095-8649.2010.02861.x>
- Rossi, V., Bernardi, M., Fornasiero, M., Nestola, F., Unitt, R., Castelli, S., and Kustatscher, E. 2024. Forged soft tissues revealed in the oldest fossil reptile from the early Permian of the Alps. *Palaeontology*, 67:e12690.
<https://doi.org/10.1111/pala.12690>
- Rothman, J.M., Chapman, C.A., Twinomugisha, D., Wasserman, M.D., Lambert, J.E., and Goldberg, T.L. 2008. Measuring physical traits of primates remotely: the use of parallel lasers. *American Journal of Primatology*, 70:1191–1195.
<https://doi.org/10.1002/ajp.20611>
- Schubert, B.W. and Ungar, P.S. 2005. Wear facets and enamel spalling in tyrannosaurid dinosaurs. *Acta Palaeontologica Polonica*, 50:93–99.
- Shearer, B.M., Cooke, S.B., Halenar, L.B., Reber, S.L., Plummer, J.E., Delson, E., and Tallman, M. 2017. Evaluating causes of error in landmark-based data collection using scanners. *PLOS ONE* 12:e0187452. Public Library of Science.
<https://doi.org/10.1371/journal.pone.0187452>
- Von Cramon-Taubadel, N., Frazier, B.C., and Lahr, M.M. 2007. The problem of assessing landmark error in geometric morphometrics: Theory, methods, and modifications. *American Journal of Physical Anthropology*, 134:24–35.
<https://doi.org/10.1002/ajpa.20616>
- Zverkov, N.G. and Jacobs, M.L. 2021. Revision of *Nannopterygius* (Ichthyosauria: Ophthalmosauridae): reappraisal of the 'inaccessible' holotype resolves a taxonomic tangle and reveals an obscure ophthalmosaurid lineage with a wide distribution. *Zoological Journal of the Linnean Society*, 191:228–275.
<https://doi.org/10.1093/zoolinnean/zlaa028>

SUPPLEMENTARY DATA

Supplementary data (3D models and template, landmarks coordinates, linear measurements, R scripts) available for download in a zipped file at <https://palaeo-electronica.org/content/2024/5265-digitisation-through-glass>.